RSC Advances

ROYAL SOCIETY OF CHEMISTRY

www.rsc.org/advances

RSC Advances

RSCPublishing

ARTICLE

Mechanisms of serpentine-ammonium sulfate reactions: Towards higher efficiencies in flux recovery and Mg extraction for CO_2 mineral sequestration.

Cite this: DOI: 10.1039/xoxxoooooox

Received ooth August 2014,
Accepted ooth

DOI: 10.1039/xoxxoooooox

www.rsc.org/

E.I. Nduagu[a]*, J. Highfield[b], J. Chen[b] and R. Zevenhoven[a],

There is a growing research interest on CO_2 mineral sequestration methods that follow an intermediate Mg extraction step (from Mg-silicates, especially serpentinite rock) by fluxing with ammonium sulfate (AS) or ammonium bisulfate (ABS). This study reports the use of thermogravimetry (TG) combined with differential scanning calorimetry (DSC), mass spectrometry (MS) and/or Fourier-transform infrared spectrometry (FTIR), to explore the serpentinite/flux [(S)/AS and S/ABS] reaction chemistry in more detail and identify conditions under which flux losses are restricted. TG-DSC-MS results show that AS decomposition proceeds through a series of reactions leading to the formation of ammonium pyrosulfate [$(NH_4)_2S_2O_7$, APS] via an ABS intermediate. That APS is the key intermediate is attested by the fact that the analogous potassium salt is a well-known flux for metal oxides. As expected the mechanisms for S/AS reaction are more complex than those of thermal decomposition of pure AS or ABS compounds. Two likely possibilities were identified with S/AS thermolysis: formation of APS or sulfamic acid (SA) precursors that extract Mg/Fe cations from serpentinite above 400°C. A sulfur dioxide peak was detected on the ensemble spectra at 280°C. This indicates a loss of ABS through sublimation rather than a complete degradation of AS or ABS reagents. At a fast heating rate of 40 K/min, tests on S/AS resulted in a significantly lower weight loss (ΔW) than at 10 K/min (46% vs. 54%), implying better retention of flux and higher extraction efficiency. From TG-FTIR tests, the presence of humidity has a suppressive effect on SA volatilization, stabilizing the hydrated intermediate APS and/or ABS. It also inhibits mineral transformation to the less reactive forsterite (Mg_2SiO_4). Extraction of magnesium is primarily dependent on serpentine particle size, but it can be increased significantly in the presence of humidity.

1 Introduction

Extraction of magnesium (as Mg^{2+} ions) from magnesium silicate rocks during mineral carbonation (also known as CO_2 mineral sequestration) is an important primary step prior to CO_2 fixation as solid magnesium carbonate ($MgCO_3$).[1-3] More recently, process routes that use ammonium sulfate (AS) or ammonium bisulfate (ABS) salts as reagents for the extraction step are gaining research attention.[4-9] One of these routes involves the reaction of Mg-silicates rocks and AS salt at 270 – 600°C to produce magnesium sulfate ($MgSO_4$),[4, 10] among other products. In a downstream process this can be carbonated, for example via $Mg(OH)_2$ as intermediate.

The reaction of serpentine [$Mg_3Si_2O_5(OH)_4$, also written as $3MgO•2SiO_2•2H_2O$] contained in serpentinite rock (S) with AS is represented as:

$$Mg_3Si_2O_5(OH)_4\,(s) + 3(NH_4)_2SO_4\,(s) \rightarrow 3MgSO_4\,(s) + 2SiO_2\,(s) + 5H_2O\,(g) + 6NH_3\,(g) \quad (1)$$

The proposed general reaction scheme (1),[4] for Mg extraction still needs verification. On the other hand, if we assume that reaction (1) correctly summarizes the overall chemical change in the S/AS reaction, the intermediate reactions and mechanisms need to be clearly identified. It has been suggested that the possible evolution of SO_2/SO_3 gases arising from thermal degradation of AS inhibits Mg extraction.[4, 7, 10] The evolution of SO_2/SO_3 gases signifies the inefficient use of AS reagent and consequently leads to low reaction conversion. Detection of SO_2/SO_3 gases in the reactor (and the gases leaving it) could indicate that the AS reagent has been completely decomposed into ammonia (NH_3), sulfur dioxide (SO_2), nitrogen (N_2) and water (H_2O).[11] In addition, the presence of SO_2/SO_3 in the reaction gases dramatically changes the equilibrium

compositions of the products leading to undesirable formation of Mg_2SiO_4 and $MgSiO_3$ instead of $MgSO_4$.[4] These imply that further investigation of the overall reaction mechanism and the possible decomposition route(s) from AS are essential if extraction efficiency is to be raised.

Knowledge of the mechanism and products of AS decomposition may provide a first indication of the chemistry occurring in the S/AS mixture. Numerous papers have reported on the thermal decomposition of AS.[12-15] However, the information is not entirely consistent. Dixon[12] reported that the residues left after heating AS to 400 °C were mainly ammonium pyrosulfate (APS) (70–73%), with minor amounts of ammonium bisulfate (ABS) (11-14%), sulfamic acid (SA) (~6%) and unreacted AS (10%). In contrast, Erdey et al.[13] reported that AS decomposes to ABS between 230 and 350°C (according to reaction (2)), and ABS is then decomposed (350 – 450°C) into sulfuric acid and ammonia gas (according to reaction (3)).

$(NH_4)_2SO_4\,(s) \rightarrow NH_4HSO_4\,(s) + NH_3\,(g)$ (2)

$NH_4HSO_4\,(s) \rightarrow H_2SO_4\,(g) + NH_3\,(g)$ (3)

Similar to the findings by Dixon [12], Halstead [14] found that at 400°C the thermal decomposition of AS salt leads to APS as the major intermediate product, which is further decomposed to gases (reactions (4)-(5)).

$2(NH_4)_2SO_4\,(s) \rightarrow (NH_4)_2S_2O_7\,(s) + 2NH_3\,(g) + H_2O\,(g)$ (4)

$3(NH_4)_2S_2O_7\,(s) \rightarrow 2NH_3\,(g) + 6SO_2\,(g) + 2N_2\,(g) + 9H_2O\,(g)$ (5)

The chemical process routes proposed by Kiyoura and Urano [15] are more complex, with the first thermal dissociation step producing ABS at 100 - 170°C (according to reaction (2)). They showed that only a partial deammoniation of the AS salt took place above 170°C, resulting in the formation of tri-ammonium hydrogen sulfate.

$2(NH_4)_2SO_4\,(s) \leftrightarrow (NH_4)_3H(SO_4)_2\,(s) + NH_3\,(g)$ (6)

This implies that any residual AS salt reacts with the newly formed bisulfate above 170°C. Contrary to the mechanism posited by Erdey *et al.*,[13] thermogravimetric (TG) analysis combined with Fourier Infrared analysis (FTIR) was used by Highfield *et al.* [7] to show that ABS decomposes up to 350 °C with no NH_3 evolution but only water vapour. The weigth loss ΔW) of ~16% was consistent with the dehydration reaction (reaction (7)):

$NH_4HSO_4\,(s) \leftrightarrow NH_2SO_3H\,(s) + H_2O\,(g)$ (7)

This is in agreement with the conclusion of Kiyoura and Urano [15], who found that the presence of water vapour inhibits dehydration. By x-ray diffraction (XRD) analysis they also showed that heating a mixture of ABS and sulfamic acid (SA) produces APS according to:

$NH_4HSO_4\,(s) + NH_2SO_3H\,(s) \leftrightarrow (NH_4)_2S_2O_7\,(s)$ (8)

Regarding the S/AS extraction mechanism, Highfield et al [7] used XRD and inductively coupled plasma atomic emission spectroscopy (ICP-AES) analysis to show that epsomite ($MgSO_4 \cdot 7H_2O$) is the final product obtained via the intermediacy of a range of Tutton salts, NH_4/Mg double sulfates. The authors identified flux loss mechanisms and found these to be substantial at 400 °C and above.

In order to gain more insight into the reaction conditions that restrict AS losses, we used the TG analysis coupled with differential scanning calorimetric and mass spectrometric analytical technique (TG-DSC-MS) to study the Mg extraction reaction as well as pure flux thermolysis. Different heating rates and gas environments were used to asses any influence of these parameters on the mineral/flux mixture, in terms of variation in the (ΔW) profiles, balance of evolved gases, etc., with implications for the Mg extraction mechanism. TG was used to study the effect of humidity on the volatilization (sublimation and/or degradation) of sulfamic acid, clearly one key intermediate in AS decomposition.[7, 12, 14, 15] Corresponding effects of humidity on the extraction efficiency and the influence of mineral particle size were also examined by TG-FTIR.

2 Experimental

The S/AS reaction chemistry was studied using a Netzsch STA 449F1 Jupiter thermogravimeter (TG)/differential scanning calorimeter (DSC) coupled to a QMS 403C Aêolos mass spectrometer (MS). TG analysis of individual samples of AS (reagent grade, >99%) and ammonium bisulfate (ABS) (reagent grade, >98%) salts, and those of Finnish serpentinite (particle size, 75 – 125 μm) mixed with AS or ABS was performed under air or helium to explore the effect of gaseous atmosphere. The amounts of materials used and the reaction conditions are presented in Table 1.

As a control, MgO (calcined Dead Sea Periclase $Mg(OH)_2$, 75 – 125 μm, purity 97.2%) was reacted with AS under similar conditions. Since Mg is present in serpentinite rock as silicate of MgO, the control test was used to identify the sensitivity of the results to other compounds, for example, Fe- and Ca-based oxides in Finnish serpentinite rock. The Finnish serpentinite rock used in the TG-MS study is a sample of the overburden from the nickel mine at Hitura and contains ~83 wt.% $Mg_3Si_2O_5(OH)_4$ and 14 wt.% iron oxides ($FeO/Fe_2O_3/Fe_3O_4$) while other trace contaminants ($CaSiO_3$, MnO, etc.) constitute 3 wt.%.[4, 7] An Al crucible (without a lid) was used as sample container for the TG tests. These were performed after achieving a uniform starting condition at 40°C through isothermal heating for 1 h followed by a dynamic heating step. Some samples were heated to 550°C at a 10 K/min heating rate while others were heated from 40 K/min to 540°C and then kept at the same temperature for 20 min.

Tests on sulfamic acid volatilization and extractions under humidity were done in an alumina crucible suspended in a Setaram Setsys S12 TG coupled to a Varian Excalibur 3000 FTIR as previously described [7], but with additional coupling to a Setaram *Wetsys* humidifier. The humidities explored here (3.6, 7.2, 10.6, and 14 vol% H_2O) were obtained by operating at 20, 40, 60, and 80% RH at 65 °C, respectively. The mineral (a lizardite/antigorite mixture according to XRD) was from a similar batch of Finnish serpentinite as for the TG-MS experiments but slightly purer in composition. XRF analysis of the mineral gave 38.1% MgO, 37.3% SiO_2, 7.5% Fe_2O_3, and 4% of other impurities (oxides of Al, Ca, Cr, Ni), corresponding to

RSC Advances RSCPublishing

ARTICLE

Table 1. Tabulated conditions and results from selected TG-DSC-MS tests

Tests	Reagent	Mass (mg)	Gas environment and heating rate	%-wt loss (at *T* °C)	*DSC* peaks (at *T* °C)	Gases released (at *T* °C)
1	AS	~25	Air 40 K/min (40-550°C)	19 (400) 99.2 (500)	340 500	NH_3,H_2O (~230) NH_3,H_2O,SO_2 (~280-290, ~410)
2	ABS	~25	Air 40 K/min (40-550°C)	11.9 (400) 99.3 (505)	160 500	NH_3 (~247). NH_3, H_2O, SO_2 (~280-290, ~450) NH_3,H_2O (~375)
3	S+AS	~12+18	Air 10 K/min (40-550°C)	15 (340) 43.4 (422) 53.5 (480)	310 410 460	NH_3,H_2O, NO (~312) NH_3,H_2O, SO_2 (~400) NH_3,H_2O,NO, SO_2 (~452-460)
4	S+AS	~12+18	Air 40 K/min (40-550°C)	13.5 (370) 35.7 (458) 47.8 (540)	NR[a] NR[a] NR[a]	NO, H_2O,NH_4 (~354-361) SO_2 (~438) NO,SO_2 (492-502)
5	S+AS	~12+18	He 10 K/min (40-550°C)	14.2 (312) 44.1 (395) 53.3 (450)	320 407 455	NH_3,H_2O (~300) NH_3,H_2O,SO_2 (350-400, 435-470)
6	S+ABS	~12+15	He 10 K/min (40-550°C)	10.6 (313) 27.7 (390) 40.9 (470)	140 360 442	NH_3,H_2O (98, 163, 400) NH_3,H_2O,SO_2 (430-460)
7	MgO+AS	~2.8+9.2	He 10 K/min (40-550°C)	15.7 (320) 44.1 (390) 50.9 (437)	295 380 430	NH_3,H_2O (300) NH_3,H_2O,SO_2 (430-460)

[a]NR – not recorded

a serpentine (phase) purity of 86%. To examine the effect of particle size on reactivity, the mineral chunks were crushed, milled, and sieved into a range of size cuts: <56, 56-125, 125-250, and 250-400 μm. Extractions were performed on 300 ± 10 mg mixtures of mineral/ammonium sulphate in a fixed weight ratio (S/AS = 0.70) as determined by the stoichiometry of reaction (1). Recovered products were analyzed by XRD in a Bruker D8 powder diffractometer with Cu Kα source (λ = 1.5418 Å) over the range 2θ = 5-80 ° at a step size of .008°. Elemental nitrogen (N) analysis was done in a Thermo Scientific Flash
2000 CHNS-O elemental analyzer. ICP-OES analyses (Mg, S, Fe) were done on a Varian Vista-MPX inductively coupled plasma optical emission spectrometer against suitably calibrated standards (5-20 ppm) on aqueous extracts from 100 mg samples diluted to 500 ml.

3 Results and discussion

3.1 MS background and evolved gas peak assignment

With increase in temperature and time, changes in the gaseous composition sampled by the MS were recorded. Positive deviations for masses (m/z) of analyte gases evolved from the mineral/flux mixture were observed. Simultaneously, negative deviations of certain "background" signals were also observed in the air flow, suggesting these are temporarily displaced by the analyte gases and confirming representative sampling. As shown in Fig. 1a, ion current curves for the principal air constituents were suppressed at *m/z* = 32, 29, 20, 16 and 14. The ion current curves for *m/z* 32 and 16 can be attributed to the molecular ion peak of dioxygen (O_2^+) and the fragment from its dissociation ionization (O^+), respectively. While coincidences at *m/z* 32 could result from SO_2^{2+} ions, which can be ruled out as unlikely contaminants. The same goes for the doubly-ionized sulfur fragment (S^{2+}) at m/z 16, e.g., from SO_2. The peak at m/z 20 is probably due to doubly-ionized argon (Ar^{2+}), the only inert gas present in air in any significant amount. The ion current curves with *m/z* 29 and 14 represent an *m*+1 peak for N_2 (or $^{15}N^{14}N^+$ nitrogen isotope peak) and the N^+ fragment ion, respectively. Turning to evolved gases from an S/AS mixture as representative, new masses were detected at m/z 17, 18, 30, 48 and 64, as shown in Fig. 1b. Ammonium ions vaporise as ammonia (NH_3 which fragments under electron impact ionization to produce three major ions at *m/z* 15 (NH^+), 16 (NH_2^+) and 17 (NH_3^+)). These signals from the ensemble mass spectrum cannot be used directly as they all suffer from significant interferences from

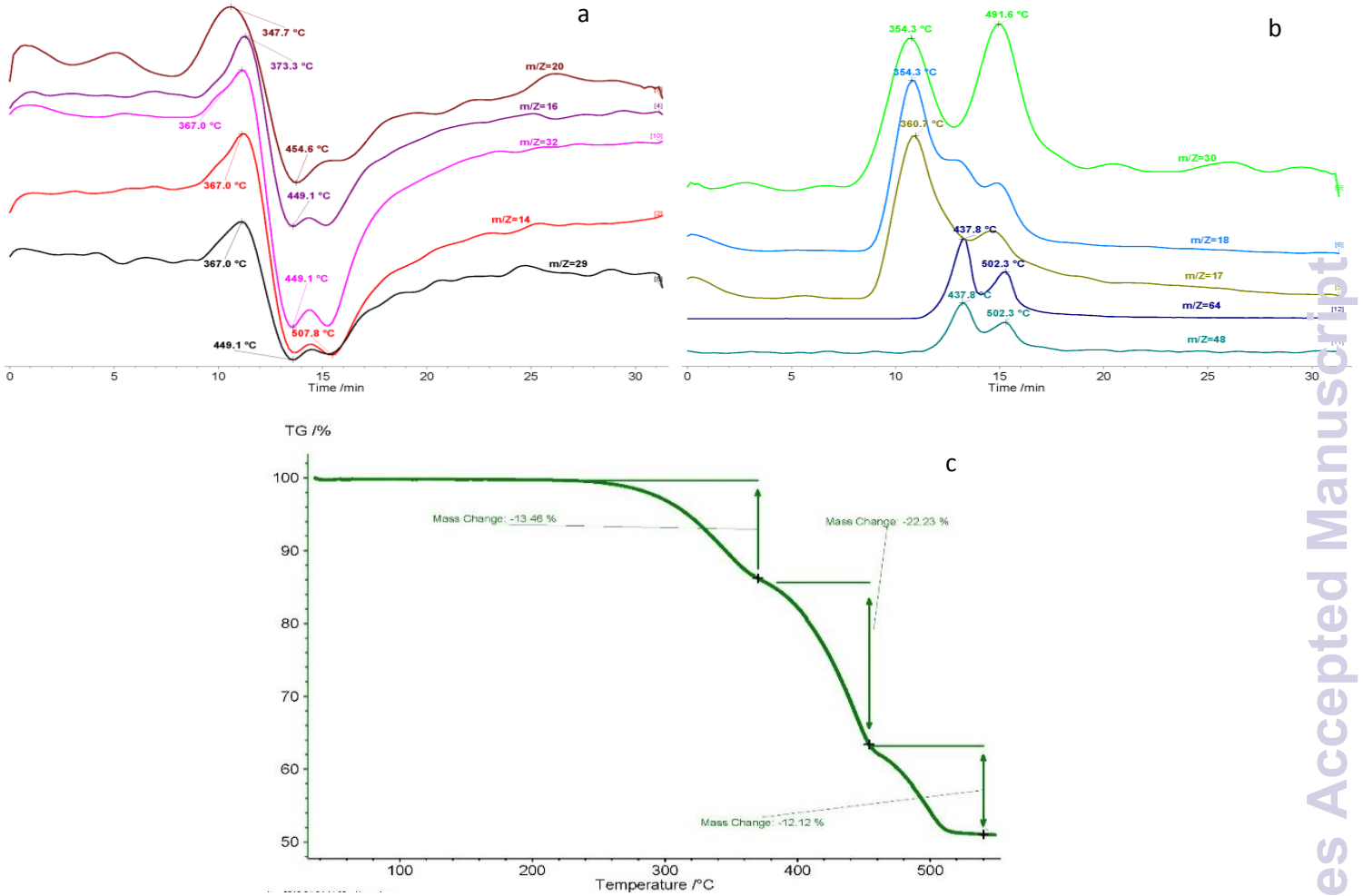

Fig. 1. a. Background MS curves. B. Evolved gas MS curves. C. TG profile. The MS and TG profiles were obtained by heating a mixture of 12 mg Finnish serpentinite and 18 mg ammonium sulfate in air from 40°C to 540°C at 40 K/min heating rate and then kept isothermally for 20 min.

other species, most notably those of $^{15}N^+$, O^+, O_2^{2+} and OH^+ ions.[16] However, the signals at *m/z* 16 and 17 can be used to determine the ammonium levels provided that the intensity contributions from the interfering species are estimated correctly. Thus, to a good approximation mass ion currents at *m/z* 17, 18, 30, 64 and 48 were taken as representing NH_3, H_2O, NO, SO_2 (and its fragment ion SO^+), respectively.

In some of the TG-MS charts in this study, the ion current curves for m/z 14, 29 and 32 are not shown when they follow similar patterns as that of m/z 16.

3.2 Thermal decomposition of AS and ABS

An understanding of the thermal decomposition of AS could provide some insights into the Mg extraction mechanism. Figure 2 shows the TG-MS charts from the thermal treatment of individual quantities of AS and ABS salts heated up in air to 540°C at a heating rate of 40 K/min and then kept isothermal for 20 min. Following the findings by Dixon [12] and Halstead [14], we hypothesize that the decomposition of AS produces APS at 400°C, but via the intermediacy of ABS product. This is based on the premise that the products of ABS degradation should be similar to the products of AS degradation above 250°C. Run under identical treatment conditions (40 K/min ramp in air), the MS spectra in Fig. 2 show that indeed the same gaseous species are released, namely, water vapor, ammonia and small amounts of SO_2 gas. The first peaks of water and ammonia appear together below 250°C but only from AS, whereas similar peaks are seen from both AS and ABS just below 300°C, suggesting they are derived from a common intermediate. The appearance of MS peaks at *m/z* 48 and 64, which can be associated with SO^+ (from SO_2) and SO_2^+ respectively, are surprising since breakdown of the flux at such a low temperature has not been reported previously. We contend that the SO^+/SO_2^+ species detected are not thermal degradation products, but derive instead from vaporized ABS that has fragmented in the MS analyzer due to electron bombardment. When enlarged, the MS spectra show very weak peaks after 400°C for the gases

RSC Advances RSCPublishing

ARTICLE

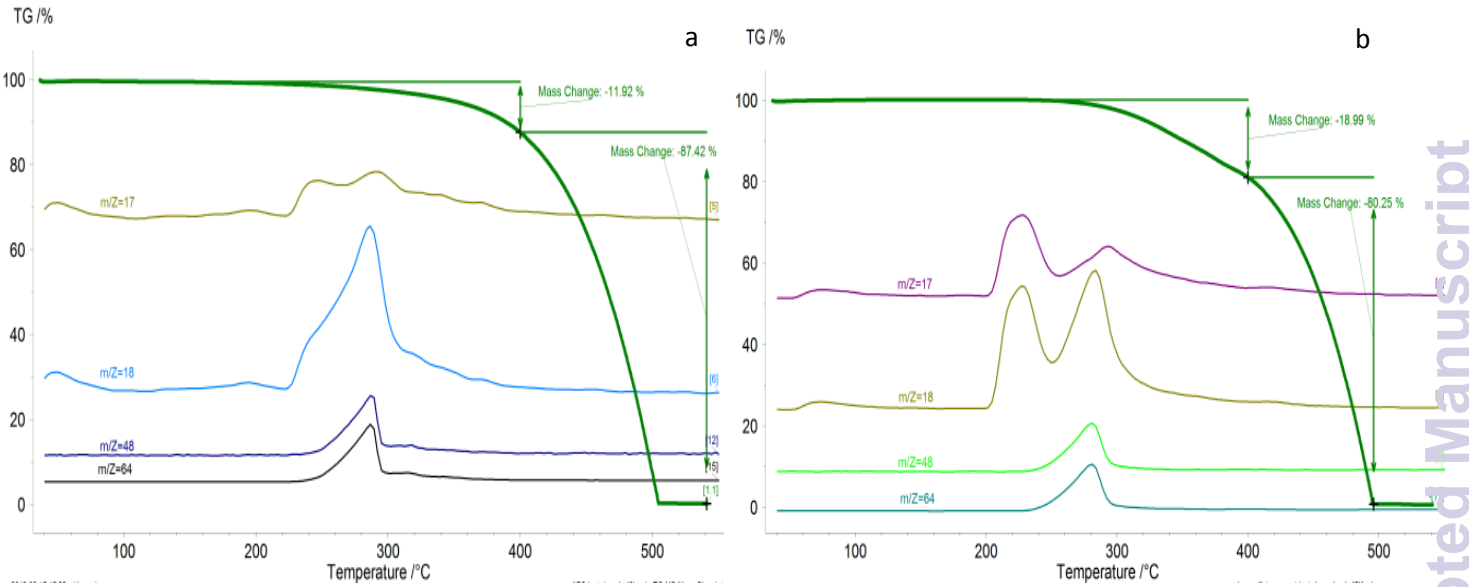

Fig. 2. a. TG-MS curves for ABS. b. TG-MS curves for AS. Reagents was heated up in air from 40°C to 540°C at 40 K/min dynamic heating rate and then kept isothermally for 20 min.

– NH_3, H_2O and SO_2. At 500°C the residues of the salt are completely decomposed.

The two major stages of gas evolution seen in MS from AS and the single stage from ABS are verified by DSC. The first major MS peaks of AS decomposition, namely, ammonia gas (*m/z* 17) and water vapor (*m/z* 18) at 230°C, can be associated with the formation of ABS. However, at this temperature no significant ΔW was observed, suggesting the true onset of AS decomposition occurs later and was complete by ~400°C. Similar to previous findings by Dixon [12] and Halstead [14], results from TG analysis show that the general mechanism of AS decomposition at 400°C can be represented as:

$$2(NH_4)_2SO_4\,(s) \rightarrow (NH_4)_2S_2O_7\,(s) + 2NH_3\,(g) + H_2O\,(g) \quad (\Delta W = -19.7\%) \quad (9)$$

$$2(NH_4)_2SO_4\,(s) \leftrightarrow 2NH_4HSO_4\,(s) + 2NH_3\,(g) \quad (\Delta W = -12.9\%) \quad (10)$$

$$2NH_4HSO_4\,(s) \leftrightarrow (NH_4)_2S_2O_7\,(s) + H_2O\,(g) \quad (\Delta W = -6.8\%) \quad (11)$$

The TG data from the decomposition of ABS and AS (Fig. 2) gave the ΔW at 400°C as ~12% and 19%, respectively. These values are quite close (with an error of <1%-points) to the stoichiometric ΔW from reactions (10) and (9), respectively. A 7%-points difference in the ΔW from the decomposition of ABS and AS corresponds (with an error of 0.2%-points) to the theoretical ΔW difference between the two. This is associated with evolution of 1 mole of water from two moles ABS (11).

Based on the assumption that the products of decomposition of ABS and AS are similar, we can conclude that the 19% ΔW at ~400°C from AS decomposition (Fig. 2) is indicative of reaction (9), which can be broken down into a series of reactions (10) and (11) leading to the formation of APS via an ABS intermediate.

3.3 S/AS reaction

The MS response during heating of the S/AS extraction mixture at 40K/min is shown versus time in Fig. 1b, along with the maximum evolution temperatures of the major peaks (marked on each plot). Between 250 and 360°C, NH_3 and H_2O were released. In addition to these gases, which were common products from AS and ABS, a mass ion peak for *m/z* 30 was also detected, indicative of NO evolution, but occurring in two stages. The first peak at 350°C was followed by a slightly stronger peak at 492°C. Previous studies of a similar mixture by TG-FTIR reported that N_2O was evolved at 350°C (as a single transitory pulse) and attributed to decomposition of SA.[7] In either case, NO_x products derive from oxidation of NH_x species and it is unlikely that these can later be recovered as NH_4^+ salts. A similar two-stage evolution was also seen for SO_2 but somewhat later at 438 and 502°C. In summary, three distinct temperature regions for peak evolution were identified at 345 - 400°C, 440°C and 480 - 520°C.

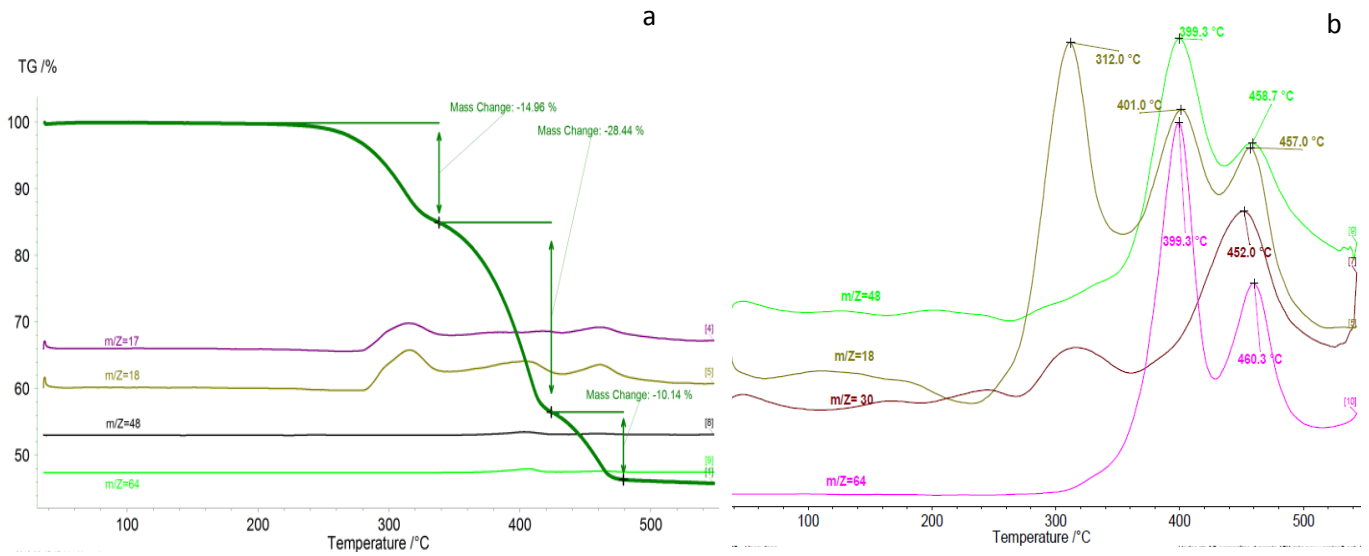

Fig. 3. S/AS reaction in air flow with 10 K/min dynamic heating from 40°C to 550°C. a) TG-MS profiles. b) Magnified MS profiles.

At a lower heating rate of 10 K/min the MS profile from the S/AS reaction is slightly different. For example, the mass ion curve for *m/z* 30, which had two distinct peaks at 40 K/min (Fig. 1b), now has one minor and one major peak (Fig. 3b). The ion current curve for *m/z* 17 was not reproduced (for clarity's sake) because it followed exactly the same pattern as the ion current curve for *m/z* 18. The mass ion curves for peaks *m/z* 17, 18, 48 and 64 (NH_3, H_2O and SO_2) were similar at both heating rates but the evolution maxima were shifted roughly by 35-50°C to lower temperature at 10 K/min. Such dynamic (inertial) effects are to be expected, becoming more pronounced at high heating rates.

The TG analyses tell a different story. Tests at both heating rates showed three distinct ΔW regions. However, 5.7 %-points more weight was lost in the test performed at 10 K/min; the total ΔW then being 53.5% (vs. 47.8%). Since these values far exceed the theoretical one (28.5% - see reaction (1)), the implication is that the high heating rate results in proportionately lower flux salt loss.This could happen if the time available for sublimation of the flux, occurring at a significant rate below the reaction temperature (with the mineral), was thereby minimized. The identified temperature regions for the TG test at 40 K/min were < 380°C, 380 - 445°C and 445 - 540°C while the associated ΔW were 13.5%, 22.2% and 12.1%, respectively. The corresponding data obtained at 10 K/min were < 340°C, 340 - 420°C, and 420 - 540°C, with associated ΔW of 15.0%, 28.4% and 10.1%, respectively. Consistent with the aforementioned view, the largest discrepancy in ΔW (6.2%) occurred during the main stage (T > 340°C) leading to onset of reaction at 400°C.

For the purpose of determining probable reaction mechanisms, the TG results at the lower heating rate (10 K/min) were considered in more detail. It was concluded in Section 3.2 that AS decomposes to APS through an ABS intermediate at about 400°C. It is of interest to know if the same reaction mechanism still applies when AS reacts with serpentine-containing rock. The production of APS from AS decomposition results in a total theoretical ΔW of 19.7%.

With the addition of 12 mg Finnish serpentinite to 18 mg AS, its decomposition corresponds to a ΔW of 13. 7%. The follow-on extraction reaction for APS can be written as:

$Mg_3Si_2O_5(OH)_4 + 1.5(NH_4)_2S_2O_7 \rightarrow$

$3MgSO_4 + 2SiO_2 + 3NH_3 + 3.5H_2O$ (ΔW = –19.2%) (12)

If Mg extraction from serpentine follows reactions (9) and (12), at ~400°C the resulting ΔW with respect to the combined weight of AS and serpentine should be 28.5%. Operating at 10K/min, we obtained a ΔW of ~34% at 400°C, as shown in Fig. 3a. This value is by far larger than the theoretical ΔW, indicating substantial loss of flux. The extraction process was also evidently incomplete at 400°C, as suggested by the discontinuity at 420°C. As already mentioned, there may be some benefit obtainable from applying a high heating ramp, like 40 K/min, a rate that is actually typical in the benchtop reactor for processing larger amounts of materials for the scale-up work. [9, 17]

The Finnish serpentinite rock used in this test also contains other reactive components (FeO, Fe_2O_3, Fe_3O_4, CaO, *etc*.) not accounted for in reactions (9)-(12). The degree to which their presence modifies the TG analysis will depend on their levels and extractability. The major impurities are Fe-oxides, constituting 14 wt.% of the rock. The balance consists of CaO (0.5 wt.%) and other impurities the effect of which can be discounted to a first approximation. A recent study [18] determined the Fe^{2+} vs. Fe^{3+} content in Finnish and Lithuanian serpentinite rocks using a wet chemical method. The study showed that Fe^{2+} constitutes 78-79% and 97% of the Fe in the Finnish and Lithuanian serpentinite rocks, respectively. If we assume that Fe is present as wüstite (FeO), the theoretical ΔW should be 13.3% according to reaction (13).

$FeO + (NH_4)_2S_2O_7 \rightarrow FeSO_4 + 2NH_3 + H_2O$ (ΔW=-13.3%)

With respect to the combined masses of Finnish serpentinite and AS reagent, reaction (13) corresponds to a 2.4% ΔW. Note that the AS reagent was supplied at an amount sufficient for 60% extraction of Fe (reaction (13)) in addition to full extraction of the Mg component (reaction (12)). Thus, for complete conversion of Mg to $MgSO_4$ and a 60% conversion of Fe to $FeSO_4$, the theoretical ΔW is ~30%. This value is still 12%-points higher than what is obtained from the TG analysis at 400ºC (Fig.1c) and ~4%-points lower than that obtained from Fig. 3a. On the other hand, with a conversion of 60% for Mg (to $MgSO_4$) and for Fe (to $FeSO_4$) as typically obtained [4], a theoretical ΔW of 17.7% is predicted. This value is very close to the 18% ΔW obtained from the TGA profile in Fig. 1c. There is, however, a possibility of another reaction taking place. We can assume that sulfamic acid (SA) could be formed from AS decomposition [7, 15] according to reaction (14):

$(NH_4)_2SO_4 \rightarrow NH_3SO_3 + H_2O + NH_3$ ($\Delta W = -26.5\%$) (14)

$(NH_4)_2SO_4 [\rightarrow NH_4HSO_4 + NH_3\ (g)] \rightarrow NH_3SO_3\ (s) + NH_3\ (g) + H_2O\ (g)$ (15)

Two major ways of producing SA from AS decomposition are through ABS or APS intermediates. Through ABS, the gaseous product compositions and theoretical ΔW remain unchanged. In this case, the formation of SA during the extraction reaction has a 15.9% ΔW with respect to the combined weight of serpentinite and AS. The SA thus produced could react with serpentine according to reaction (16):

$3NH_3SO_3 + Mg_3Si_2O_5(OH)_4 \rightarrow 3MgSO_4 + 2SiO_2 + 3NH_3 + 2H_2O$ ($\Delta W = -15.3\%$) (16)

$FeO + NH_3SO_3 \rightarrow FeSO_4 + NH_3$ ($\Delta W = -10.0\%$) (17)

With respect to the serpentinite rock and AS reactant, the combined ΔW from reactions (15) and (16) is 26.4%. If we postulate that the reaction of FeO with SA is accompanied by a de-ammonization reaction according to reaction (17), then the resulting ΔW is 0.8%, which is of only minor significance. This brings the cumulative ΔW for the reaction of SA (formed via the ABS precursor) and serpentinite to 27.2%. When we account for inefficient (60%) Mg and Fe extraction reactions, the predicted ΔW should be between 16.6% and 21.9%. The result obtained in Fig.1c also fits quite well into an AS→SA intermediate route. However, the fit to the AS→APS intermediate route is better.

On the other hand, SA can be produced from an APS precursor according to:

$(NH_4)_2S_2O_7 \rightarrow 2NH_3SO_3\ (s) + H_2O\ (g)$ ($\Delta W = -8.5\%$) (18)

The theoretical ΔW with respect to the initial reactants (serpentinite/AS), is 25.5%. The reaction of Fe with AS reagent is accompanied by the de-ammonization reaction (17) with a ΔW of 0.8%, resulting in a total ΔW of 26.3%. When we account for inefficient Mg and Fe extraction, the predicted ΔW should range from 15.9% to 21.2%.The effect of helium gas on the S/AS reaction was also examined. There was a significant change in the TG-MS results when the reaction was performed in an inert gas flow environment, as seen by comparing MS traces in Fig. 4 (He) vs. Fig. 3 (air). Analytically, the use of He carrier gives rise to a substantial improvement in data quality. Background (interference) peaks (not shown) are minimized, leading to more distinctive analyte peaks at *m/z* 16, 17, and 18. For example, in the absence of O_2, the *m/z* 16 peak now reflects the level of NH_2^+, evolving at the same temperature as *m/z* 17 (NH_3^+) as expected. Furthermore, the NO (*m/z* 30) peak is absent in He, proving that it originates from a reaction of NH_x species with molecular O_2. Curiously, all spectral peaks were found at systematically lower temperatures in He as compared to air flow, the first peak occurring at 300°C (vs. 312ºC in air). At the same heating rates (10 K per min), very similar total ΔW (52-53%) were measured, but reactions in He were complete by 455°C (vs. 480°C in air). This shift to lower temperature was evident also in the individual ΔW stages. In Fig. 4, these were < 313ºC ($\Delta W = -12.2\%$), 313-395ºC ($\Delta W = -30.0\%$) and 396-455ºC ($\Delta W = -9.25\%$).

DSC peaks at 280°C, 360°C, and 425°C were consistent with the respective maxima in the derivative ΔW. The corresponding values in air were < 340ºC ($\Delta W = -15.0\%$), 340-420ºC ($\Delta W = -28.4\%$), and 420-540ºC ($\Delta W = -10.1\%$). It remains unclear if the apparent inhibitory effect of air is of chemical or physical origin, but the latter is most probable. It is known that the thermal diffusivity of air is much lower than that of He, thereby adding more thermal inertia (delay in thermal equilibration at the sample) during a ramp. The production of SO_2 is considered to mark the onset of decomposition of AS, which reduces the efficiency of the extraction reactions. Almost regardless of gas atmosphere, this occurs just below 400°C, consistent with the value of ~390°C identified in our previous study.[7]

3.4 S/ABS reaction

The DSC curve for S/ABS reaction in He flow (Fig. 5) appears to be "missing" the first peak at 280°C as seen in the S/AS reaction. However, other low temperature features are evident, namely, minor endothermic peaks at 90 and 145ºC, accompanied by small MS peaks for H_2O (*m/z* 18, 17). The first is removal of adventitious absorbed water (ABS is hygroscopic), whereas the 145°C endotherm is probably due to sudden residual water release triggered by ABS melting.

However, a weak "background" signal of water continued up to 300°C, at which point a quasi-continuous ΔW up to ~10% had been measured.

RSC Advances RSCPublishing

ARTICLE

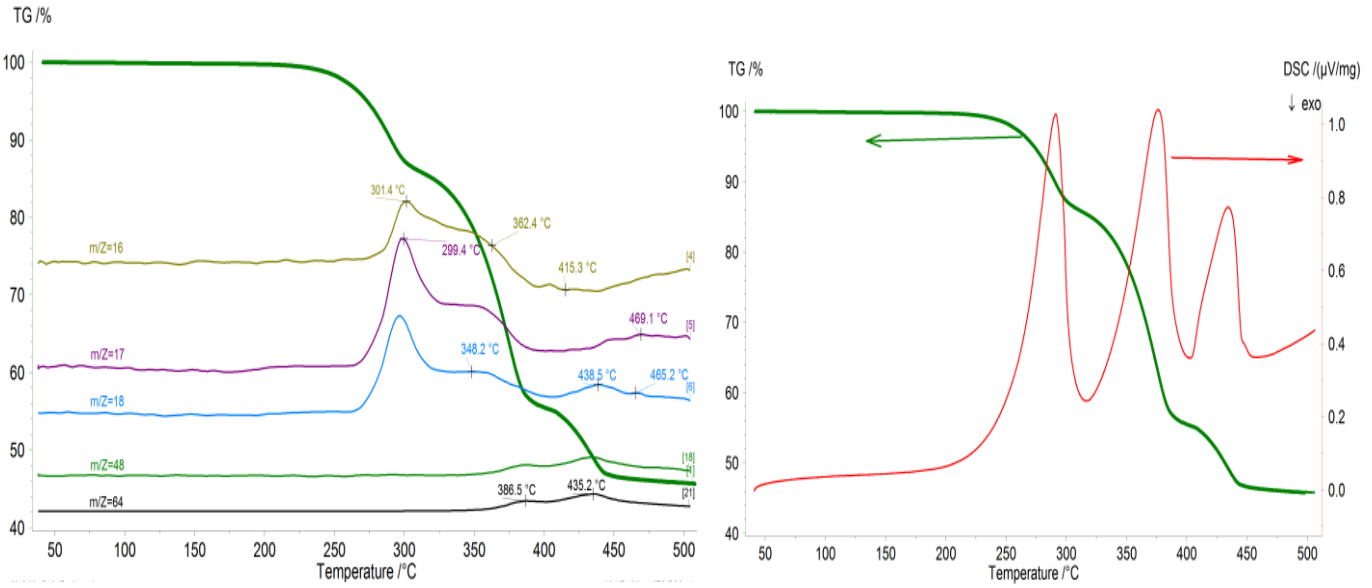

Fig. 4. S/AS reaction in He flow with 10 K/min heating ramp: 40°C to 540°C. *Left:* TG-MS profiles. *Right:* TG-DSC profiles.

If reaction (11) is followed, APS is the product with a predicted ΔW (with respect to the combined masses of serpentine and ABS) of 4.3%. However, the actual ΔW was closer to that for ABS dehydration to SA, with a theoretical ΔW of 8.7%. If this is the case, extraction by SA can be written as:

$$3NH_3SO_3 + Mg_3Si_2O_5(OH)_4 \rightarrow 3MgSO_4 + 2SiO_2 + 3NH_3 + 2H_2O \quad (\Delta W = 15.3\%.) \quad (19)$$

with a theoretical ΔW of 15.3%. This is similar to the actual 2nd stage ΔW (310-400°C) of 17.1%. New peaks of NH_3 and H_2O just below 400°C, corresponding with the DSC peak at ~360°C, all appear to support assignment of the 2nd stage to extraction chemistry. The third stage beyond 400°C (DSC peak at 440°C) had associated NH_3/H_2O peaks, but also showed the familiar MS responses at *m/z* 48 and 64 (SO_2 evolution), confirming flux decomposition.

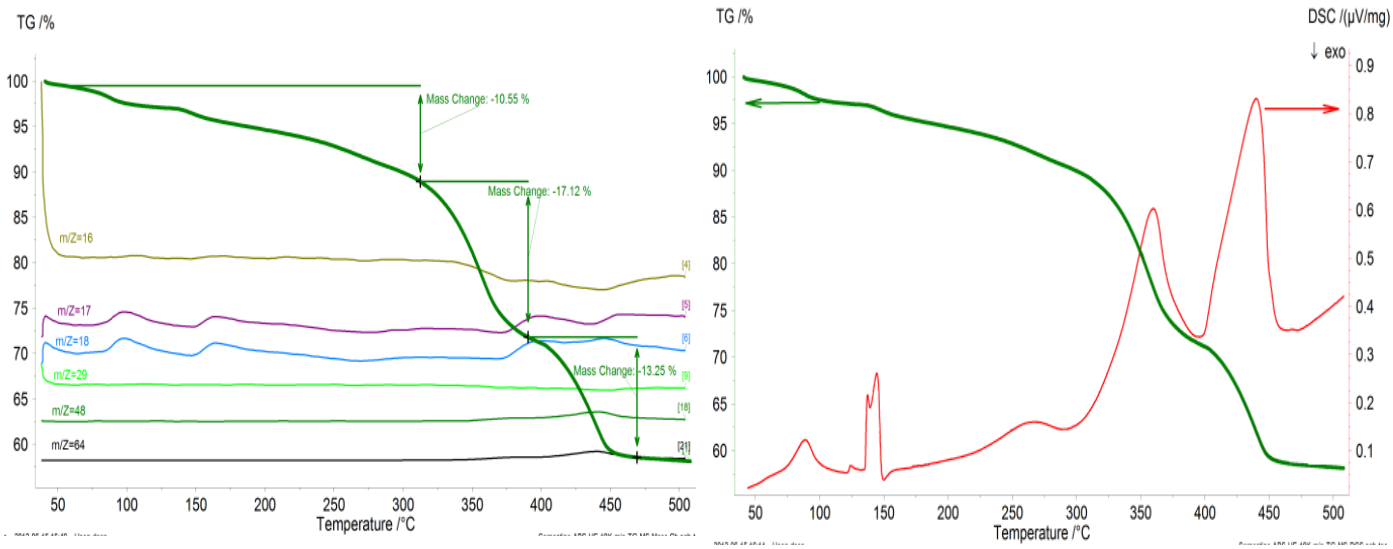

Fig. 5. S/ABS reaction in He flow and 10 K/min heating ramp: 40 to 550°C. *Left*: TG- MS profiles. *Right*: TG-DSC profiles.

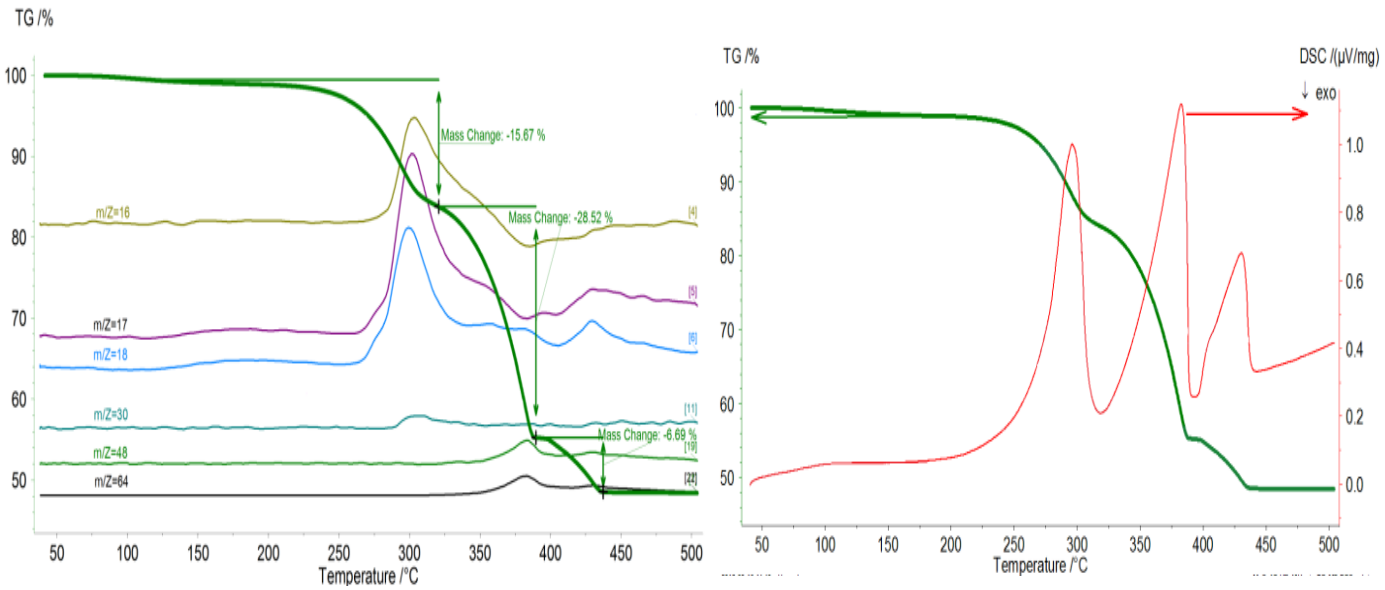

Fig. 6. MgO/AS reaction in He gas flow and 10 K/min dynamic heating from 40 to 550°C. *Left:* TG- MS profiles. *Right:* TG-DSC profiles.

Once again, the overall ΔW (> 40%) exceeded significantly the expected value of 22.7%, for the S/ABS reaction, showing that flux losses are relatively similar in both AS and ABS.

3.5 MgO/AS reaction

TG-DSC-MS analysis on the MgO/AS reaction was performed as a control test. Results should highlight the more intractable mineral environment in the S/AS reaction, including the effect of impurities. The TG-MS and TG-DSC profiles for MgO/AS (Fig. 6) and S/AS reactions (Fig. 4) were very similar. The first sign of SO_2 evolution occurs below 400°C while the final degradation stage of AS peaks at 430°C with the evolution of H_2O, NH_3, SO_2, and NO. The theoretical ΔW for the MgO/AS reaction is 30.2% as below:

$$3MgO + 3(NH_4)_2SO_4 \rightarrow 3MgSO_4 + 6NH_3 + 3H_2O \quad (\Delta W = -30.2\%) \quad (20)$$

which is very similar to that of the S/AS reaction (28.5%). The formation of ABS at 250-330°C corresponds to ΔW = 9.9% with respect to the MgO/AS mixture, whereas the TG data gives ΔW = 15.7%. The "extra" loss (5.8%) appears to correlate with H_2O evolution, suggesting dehydration to APS (5.2%) and/or SA (10.4%), although ABS sublimation may contribute to the total (see Fig. 5). Curiously, Fig. 6 shows the presence of a weak NO peak (*m/z* 30) at 300°C. This may result from preferential oxidation of any sublimate due to its highly dispersed form, but its absence in the S/AS reaction via the same mechanism cannot be explained. TG results show a second stage ΔW of 28.5% at 325-390°C (Fig. 6), bringing the cumulative ΔW to 44.2%. At this point, it is expected that the formation of APS (or SA) from AS and its reaction with MgO:

$$2MgO + (NH_4)_2S_2O_7 \rightarrow 2MgSO_4 + H_2O + 2NH_3. \quad (\Delta W = -17.7\%) \quad (21)$$

is complete, but this sums to reaction (20), or a loss of 30.2%. Thus, even before the 3rd stage (ΔW ~7%) representing final gasification at 440°C, a significant flux loss has already occurred. The potential importance of SA and its inter-relationship with ABS and APS by humidification are considered in Section 3.6.

3.6 TG and TG-FTIR studies of sulfamic acid volatilization and effect of humidity

From a preliminary test on sulfamic acid (SA) by TG-FTIR in a dry N_2 flow up to 500°C, 3 stages of volatilization were identified as seen in Fig. 7a. Below 300°C it merely sublimed, losing up to 20 wt% but with no detectable other evolved gas. From 300-400°C, NH_3 and H_2O were evolved with a stage ΔW of ~25%, suggesting decomposition to pyrosulfurous acid:

$$4NH_3SO_3 \rightarrow 2H_2S_2O_5 + 2NH_3 + 2H_2O + N_2 \quad (\Delta W = -25.3\%) \quad (21)$$

Any N_2 produced would be undetectable by IR spectroscopy. Above 400°C, SO_2 and H_2O were released together according to:

$$H_2S_2O_5 \rightarrow 2SO_2 + H_2O \quad (22)$$

In earlier work [19], Halstead proposed a very complex degradation mechanism in which SO_3 is initially a minor component but this was not substantiated by FTIR as no S=O band was seen at 1400 cm^{-1}.[20]

In separate TG experiments, a ramp and hold at a typical extraction temperature of 400°C resulted in volatilization of the entirety of the SA sample within 30 minutes, implying severe competition between extraction and flux loss. In contrast, with 3.6 vol% H_2O present at a lower temperature (200°C), a weight gain plateau of 17.0% was reached in one

hour, suggesting that ABS is formed, presumably being the more stable intermediate under these conditions:

NH_3SO_3 (s) + H_2O (g) ←→
NH_4HSO_4 (s) (ΔW=+17.5%) (23)

At 300 °C and the same humidity level, a weight gain was still observed during the ramp stage but it passed through a maximum, dropping slowly to ~9% within 2 hours. This suggests that SA now transforms to APS according to:

$2NH_3SO_3$ (s) + H_2O (g) ↔
$(NH_4)_2S_2O_7$ (ΔW = + 8.8%) (24)

for which the theoretical weight gain is 8.8%. However, by 350 °C, there was a continuous ΔW at a fixed rate of ~17% per hour. The effect of varying the humidity (vs dry N_2 control) at 400°C is shown in Fig. 7b. During the ramp stage, weight gains of up of 10-12% were initially seen at all humidities. However, during the final hold steady ΔW levels were established whose slopes were dependent on the humidity level. It can be concluded that material losses occur primarily via a physical mechanism, namely, sublimation, because in all cases fixed rates were maintained down to an abrupt discontinuity at 100% loss (not shown). Unlike previous TG-FTIR studies [7] that confirmed sublimation (and re-solidification downstream) as the cause of blocked tubing, the same instrumental problem was avoided here by prior disconnection of the transfer line to the FTIR. The differing slopes may reflect the susceptibility to sublimation

a b

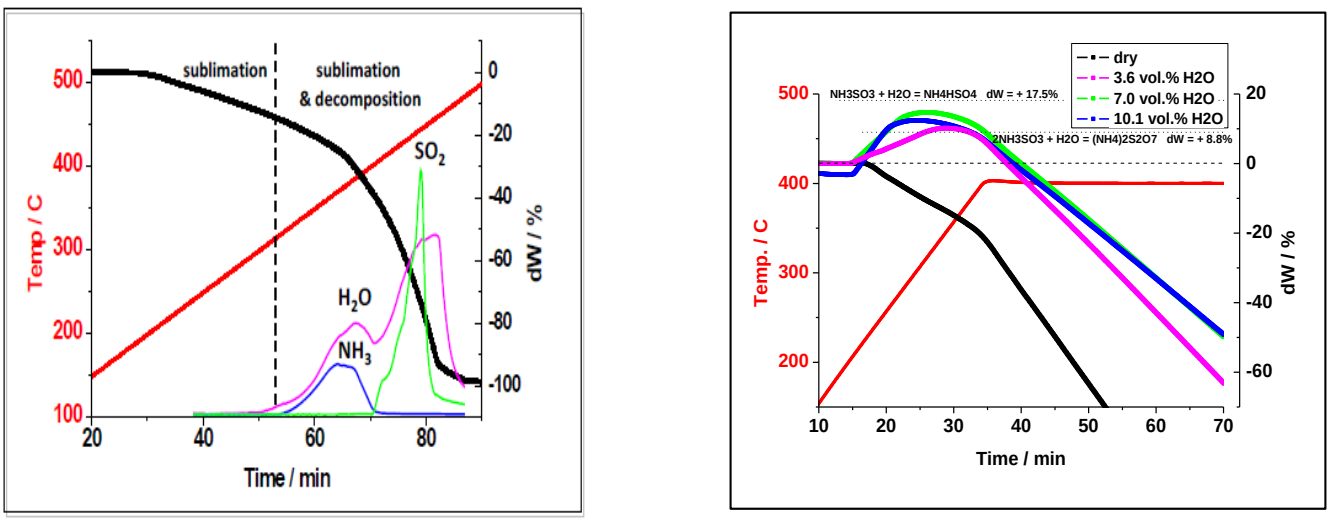

Fig.7. (a) TG-FTIR of sulfamic acid up to 500 °C in dry N_2 (b) Effect of humidity on TG curves up to 400 °C

a. b.

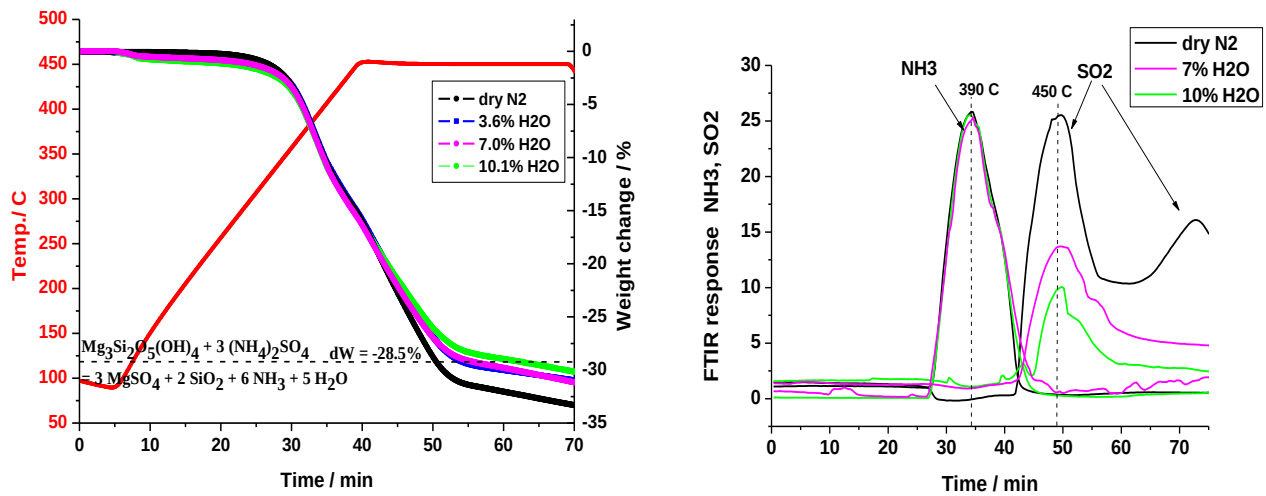

Fig. 8. Effect of humidity on (a). TG curves for reaction of Finnish serpentine with ammonium sulfate up to 450°C; and (b). NH_3 and SO_2 evolution in the same experiments by FTIR

of stabilized (more hydrated) intermediates ABS and APS, and/or equilibrium mixtures with SA.

Typically, the presence of water vapour restricted the volatilization rate to just 60% per hour, suggesting a far longer contact time between flux and mineral may be achieved, with benefits for extraction efficiency. The effect of the same levels of humidity on extraction up to 450°C, as indicated by the TG curves for fine particle size Finnish serpentinite (< 56 μm) in admixture with a stoichiometric amount of ammonium sulfate (S/AS = 0.70), are shown in Fig. 8a. A baseline ΔW of 33% was recorded in dry N_2 but increasing levels of humidity caused a progressive increase in the final weight of the residue, suggestive of restricted loss of flux and, potentially, improved extraction of Mg. At 14 vol% H_2O, the ΔW approached 30%, i.e., very close to the theoretical value for 100% extraction from pure serpentine (reaction (1), ΔW = –28.5%), as marked by the dashed line. The effects of humidity on the FTIR response for NH_3 and SO_2 evolution during the same experiments are shown in Fig. 8b. Ammonia was released first, peaking at roughly 390°C, whereas SO_2 was evolved in two stages at 450°C in dry N_2, suggesting a complex decomposition mechanism. While NH_3 evolution was unaffected by the presence of humidity, the loss of SO_2 was progressively limited although it never reached zero even at the highest humidity level explored. The loss mechanism for sulfamic acid, the inevitable product in dry carrier gas, is evidently a combination of sublimation and degradation to gaseous products. The simplest interpretation is that humidity promotes formation of $(NH_4)_2S_2O_7$, probably the most thermally stable and least volatile flux component. This view is supported by the fact that the related potassium salt, a common flux used in mineral dissolution (XRF analysis), does not start to evaporate significantly until above 500°C.[21]

TG curves for coarser particle cuts (56-125 μm and 250-400 μm) showed clear evidence for progressively higher losses, the weight changes in dry N_2 under similar conditions being –41 and –55%, respectively. On the simple assumption that the flux can either extract Mg (as $MgSO_4$) or volatilize away uselessly, a hypothetical ΔW can be a calculated for any degree of extraction on the basis of material balance. The foregoing (measured) ΔW values correspond to 86, 58, and 14% Mg, respectively. As shown in Table 2, the addition of humidity restricted the ΔW substantially, resulting in a hypothetical doubling of extraction for the large (250-400 μm) particle fraction. Best estimates of extraction levels of Mg and recovery level of S from wet chemical analysis (ICP) are also listed. Further information given in Table 2 includes product (phase) composition by XRD and elemental N analysis (as a measure of residual NH_4^+ ion).

The first encouraging result in the finest (< 56 μm) mineral extractions was the recovery of the flux, as estimated from the S level determined by ICP. This ranged from 82% (dry N_2) up to 91% (14 vol% H_2O), and substantially higher than reported previously.[7] These values of S recovery were quite consistent with the Mg extraction values predicted by gravimetry. However, the actual (soluble Mg) levels by ICP were found to be consistently lower than the S recoveries, suggesting the formation of Mg products containing "excess" sulfate (vide infra). The fact that a high (S)ulfate recovery was obtained even from extraction under dry N_2 shows that mineral particle size is a very important determinant of flux recycling efficiency. A growing discrepancy was seen between hypothetical extraction of Mg (as indicated by TG) and S recovery (by ICP) with increasing particle size. The predictive power of the measured weight loss then became quite poor, presumably due to increasing deviation from the simplistic assumptions

Table 2 - Results of extractions on Finnish serpentinite (1/3 mol/mol mix with ammonium sulfate)

grain size (μm)	extraction temp/time [°C /min]	gas flow humidity (% H_2O)	product phase(s) XRD	wt loss (%) TG	% N (EA)	% Mg extr.‡ [TG]	% Mg extr. ICP	% S extr. ICP
< 56	450/30	0 (N_2)	$(NH_4)_2Mg_2(SO_4)_3$ [$MgSO_4$•$7H_2O$]* > SiO_2 (?) > $MgSO_4$•$6H_2O$ ≈ $(NH_4)_2Mg(SO_4)_2$•$6H_2O$ > $[Mg(Fe)]_2SiO_4$ (I = 3300)	33	2.26	86	54	82
		7.2		31	—	92	55	85
		10.6	as dry N_2 but less Forsterite $[Mg(Fe)]_2SiO_4$ (I = 2900)	31	—	92	56	88
		14.0		30	2.45	95	58	91
56-125	430/45	0 (N_2)	as fine grain (< 56 μm) but Forsterite now strongest pattern $[Mg(Fe)]_2SiO_4$ (I = 4600)	41	1.83	58	21	27
		7.2		37	—	75	23	31
		10.6		36	—	77	24	32

		14.0	as dry N_2 but less Forsterite $[Mg(Fe)]_2SiO_4$ (I = 2000)	32	2.27	85	26	36
250-400	450/30	0 (N_2)		55	0.97	14	7	10
		10.6		51	2.00	27	13	22

‡ Estimated from wt loss data * after exposure to air: $(NH_4)_2Mg_2(SO_4)_3 + 13H_2O \rightarrow MgSO_4{\bullet}7H_2O + (NH_4)_2Mg(SO_4)_2{\bullet}6H_2O$

made as regards material balance. The effect of heat treatment regime on reaction progress was examined briefly in dry N_2 for the intermediate (56-125 μm) particle size but found to be quite minor. The tabulated values of 21% Mg extraction and 27% S recovery for this slightly lower temperature/longer time treatment were comparable to the values obtained after heating to 450 °C for 30 minutes, namely, 22% and 29%, respectively.

The more puzzling result in Table 2 is the extraction efficiencies for Mg. These remained at quite modest levels (< 60%), similar to those reported in our earlier work [4, 7, 9, 10], despite excellent stabilization of the flux in the fine particle mineral size fraction. XRD analysis provides one possible explanation insofar as the dominant extracted phase was $(NH_4)_2Mg_2(SO_4)_3$, also known as synthetic efremovite. If this is an essential intermediate in the mechanism (ultimately yielding $MgSO_4$ or its hydrates), then the stoichiometry of reaction 1 corresponds to a 50% deficit in the amount of flux needed for full extraction:

$$^2/_3Mg_3Si_2O_5(OH)_4 + 3(NH_4)_2SO_4 \rightarrow (NH_4)_2Mg_2(SO_4)_3 + {}^4/_3SiO_2 + {}^{10}/_3 H_2O + 4NH_3 \quad (25)$$

resulting in a theoretical maximum Mg extraction level of 67%. The actual process is not represented exactly by reaction (25) because the associated ΔW (22.6%) was well exceeded and the next most intense pattern in XRD was that of hexahydrite ($MgSO_4{\bullet}6H_2O$). Equilibration of the samples in ambient air over several days resulted in a significant weight gain (> 50%) and dramatic changes in XRD, efemovite and hexahydrite being replaced mainly by epsomite [$MgSO_4{\bullet}7H_2O$] and with some growth in boussingaultite [$(NH_4)_2Mg(SO_4)_2{\bullet}6H_2O$], suggestive of a disproportionation reaction:

$$(NH_4)_2Mg_2(SO_4)_3 + 13H_2O \rightarrow MgSO_4{\bullet}7H_2O + (NH_4)_2Mg(SO_4)_2{\bullet}6H_2O \quad (26)$$

The previous assignment of a peak at 2θ ≈ 10.8 ° to SiO_2 [7] may have been in error. Although this peak appeared regularly in these experiments and silica is an expected product, exposure to ambient air caused substantial weakening of its intensity. Other frequent and significant peaks difficult to assign were seen at 2θ ≈ 24.2 ° (d = 3.69 Å), 30.6 ° (d = 2.92 Å), and a doublet around 62.5 ° (d = 1.48 Å), the last present only in the 250-400 μm mineral cut. As they were also more intense in these coarser particles, they probably derive from a non-hydrated serpentinite structure akin to olivine produced in-situ. No evidence was seen for residual (mainly lizardite) mineral or unreacted AS, which would have been indicated by their respective main peaks at 2θ ≈ 12.1° (d = 7.31 Å) or 26.6° (d = 3.35 Å), respectively. Also absent were the peaks of probable intermediates APS (2θ ≈ 17.6°, d = 5.02 Å), ABS (2θ ≈ 18.7°, d = 4.75 Å), or SA (2θ ≈ 22.1°, d = 4.01 Å).

More information on the solid product composition was gleaned from the N analysis, which at around 2.5 wt% N was roughly half that expected (5.5 wt%) if all the flux was assumed to have formed efremovite. Despite the evidence that a significant fraction of Mg was not extracted due to flux limitation, no starting mineral (antigorite) was seen in XRD. Instead, the patterns of forsterite/fayalite [olivine - $\{Mg(Fe)\}_2SiO_4$], accounted for residual Mg and Fe, the principal contaminant. This is a surprising observation because dehydroxylation of the heated serpentinite mineral alone normally occurs well above 500 °C.[22-24] Furthermore, it yields an amorphous dehydrated "meta-serpentinite" phase that is more reactive with CO_2, forsterite only crystallizing out at close to 800 °C. Thus, the presence of the flux not only initiates Mg extraction but at the same time accelerates reaction 27:

$$2Mg_3Si_2O_5(OH)_4 \rightarrow 3Mg_2SiO_4 + SiO_2 + 4H_2O \quad (27)$$

a complex process involving phase segregation. Since treatment in dry N_2 resulted in higher forsterite levels (see Table 2 - XRD intensity (I) values in parentheses), the suppressing effect of water on this undesirable side reaction was doubly important. The observed trend of increasing forsterite product from the larger mineral particle size (lower extraction) under otherwise identical conditions would also be expected because of the limited-time (partial) access of the flux to the mineral core.

Conclusions

This paper addresses the mechanisms of Mg extraction from Finnish serpentinite rock using recoverable AS reagent for the purpose of CO_2 mineral sequestration. Having a closed loop process necessitates that AS reagent losses are restricted ideally to zero. Therefore, identifying the loss mechanisms and establishing reaction conditions that minimize losses are important. We believe that the power of the coupled thermal-spectroscopic methods applied towards these objectives, namely, thermogravimetry (TG)/ differential scanning calorimetry (DSC) – mass spectrometry (MS) and TG-FTIR, is self-evident.

Similar to previous literature, we conclude that AS reagent first decomposes to ABS between 200°C and 250°C, releasing ammonia (NH_3) gas and water (H_2O) vapor. Sulfur dioxide gas was detected at 250 - 320°C, marking a second mechanism of AS loss. A similar occurrence was observed

with tests performed on the thermal decomposition of ABS. Detection of an SO_2 peak in this temperature range indicates a loss of ABS through sublimation rather than a complete degradation of AS or ABS. It was concluded that AS decomposition proceeds through a series of reactions that lead to the formation of APS via an ABS precursor. Weight loss calculations show that by 400°C APS is the predominant product of AS and ABS decomposition, and thus, the most likely reagent for Mg and Fe extraction from serpentinite in the range 400 - 480°C.

On another hand, qualitative and quantitative interpretation of thermolysis of the S/AS reaction is not as straightforward as that of pure AS or ABS compounds. The likely possibilities were identified with S/AS tests: formation of APS or sulfamic acid (SA) precursors that extract Mg/Fe cations from serpentinite above 400°C. However, the reaction of serpentinite with the APS precursor was found to be the most probable. At a heating rate of 10 K/min, tests performed with S/AS show a first peak of SO_2 at 400°C and a second peak at 435°C, while at a 40 K/min heating rate the first and second peaks of SO_2 are distinct at 437 and 502°C respectively. In addition, applying the faster heating rate in the S/AS reaction results in a significantly lower weight loss than at 10 K/min, namely, 46% vs. 54%, respectively, implying better retention of flux and higher extraction efficiency. Thus, heating rates ≥ 40 K/min should be further explored as one means to minimize AS reagent losses at identified optimal Mg extraction temperatures of 440 - 480°C. Other process variables that offer benefits in terms of flux recovery and Mg extraction are milling to fine particle size and the use of humid gas flow, which stabilizes less volatile flux components and the more reactive serpentine (hydrated) mineral form of magnesium silicate.

Acknowledgements

This work was part of activities in the joint project "Novel Low Energy Routes to Activate Minerals for Large-scale Carbonation for Useful Products" (2010-2014) with partial funding by the Finnish Funding Agency for Technology and Innovation (TEKES) and Singapore's Agency for Science, Technology and Research (A*Star).

List of Abbreviations

Abbrev.	*Meaning*	*Formula*
ABS	Ammonium bisulphate	NH_4HSO_4
APS	Ammonium pyrosulphate	$(NH_4)_2 S_2O_7$
AS	Ammonium sulphate	$(NH_4)_2SO_4$
DSC	Differential Scanning Calorimetry	
FTIR	Fourier-transform infrared spectrometry	
ICP-AES	Inductively Coupled Plasma Atomic Emission Spectroscopy	
ICP-OES	Inductively Coupled Plasma Optical Emission Spectrometry	
MS	Mass Spectrometry	
S	Serpentinite	$(Mg,Al)_3[(Si,Fe)_2O_5](OH)_4$
SA	Sulphamic acid	NH_3SO_3
TG	Thermogravimetry	
XRD	X-ray diffraction	
XRF	X-ray Fluorescence	
ΔW	Weight loss (%)	

Notes and references

[a] Thermal and Flow Engineering, Åbo Akademi University, Biskopsgatan 8, 20500, Turku, Finland.

[b] Institute of Chemical and Engineering Sciences, ICES/A*Star, Singapore

* corresponding author, currently at Department of Chemical and Petroleum Engineering, University of Calgary, Calgary, Alberta Canada, e-mail: einduagu@ucalgary.ca.

1. K.S. Lackner, *Annu. Rev. Energy Environ*. **2002,** *27*, 193-232.
2. K.S Lackner, D.P. Butt, C.H. Wendt, *Energ Convers. Manage.* **1997,** *38*, 259-264.
3. R. Zevenhoven, S. Teir, S. Eloneva, *Energ*, **2008,** *33*, (2), 362-370.
4. E. Nduagu, T. Björklöf, J. Fagerlund, J. Wärnå, H. Geerlings and R. Zevenhoven, *Miner. Eng.*, **2012,** *30*, 75-86.
5. X. Wang and M. M. Maroto-Valer, *ChemSusChem.* **2011,** *4*, (9), 1291-1300.
6. X. Wang and M. Maroto-Valer, *Energy Procedia*, **2011,** *4*, (0), 4930-4936.
7. J. Highfield, H. Lim, J. Fagerlund and R. Zevenhoven, *RSC Adv.*, **2012,** *2*, 6535-6541.
8. R. Zevenhoven, J. Fagerlund and J. K. Songok, *Greenhouse Gases Sci. Technol.*, **2011,** *1*, (1), 48-57.
9. I.S. Romão, L.M. Gando-Ferreira and R. Zevenhoven, *Miner. Eng.*, **2013**, *53*, 167-170
10. E. Nduagu, T. Björklöf, J. Fagerlund, E. Mäkilä, J. Salonen, H. Geerlings and R. Zevenhoven, *Miner. Eng.*, **2012,** *30*, 87-94.
11. Y. Liske, S. Kapila, V. Flanigan, P. Nam and S. Lorbert, *J. Hazard. Subs. Res.*, **2000,** *2*, 8-1 - 8-17.
12. P. Dixon, *Nature* **1944,** *154*, 706.
13. L. Erdey, S. Gal and G. Liptay, *Talanta*, **1964,** *11*, (6), 913-940.
14. W. Halstead, *J. Appl. Chem.*, **1970,** *20*, (4), 129-132.
15. R. Kiyoura and K. Urano, *Ind. Eng. Chem. Process Des. Dev.*, **1970,** *9*, (4), 489-494.
16. J. D. Allan, A. E. Delia, H. Coe, K. N. Bower, M. R. Alfarra, J. L. Jimenez, A. M. Middlebrook, F. Drewnick, T. B. Onasch and M. R. Canagaratna, *J. Aerosol Sci.*, **2004,** *35*, (7), 909-922.
17. Nduagu, E. PhD Thesis, Åbo Akademi University Turku, Finland, 2012. Available at <http://www.doria.fi/handle/10024/86170> (Accessed 15.8.2014).
18. E. Koivisto, MSc. Thesis, Luleå University of Technology, Sweden, 2013.
19. W. D. Halstead, *J. Appl. Chem.*, **1971,** *21*, 22-26.
20. A. Given, A. Loewenschuss, C. J. Nielsen and M. Rozenberg, *J. Mol. Struct.*, **2007**, *830*, 21-34.
21. K. J. De Vries and P. J. Gellings, *J. Inorg. Nucl. Chem.*, **1969**, *31*, 1307-1313.
22. M. J. McKelvy, A. V. G. Chizmeshya, J. Diefenbacher, H. Béarat, and G. Wolf, Environ. Sci. Technol., **2004**, *38*, 6897-6903.
23. R. D. Balucan and B. Z. Dlugogorski, Environ. Sci. Technol., **2013**, *47*, 182-190.
24. R. D. Balucan, B. Z. Dlugogorski, E. M. Kennedy, I. V. Belova, G. E. Murch, Int. J. Greenhouse Gas Control **2013**, *17*, 225-239.

